sensors

MDPI

Article

Oxygen- and pH-Dependent Photophysics of Fluorinated Fluorescein Derivatives: Non-Symmetrical vs. Symmetrical Fluorination

Ciaran K. McLoughlin [1], Eleni Kotroni [2], Mikkel Bregnhøj [1], Georgios Rotas [2], Georgios C. Vougioukalakis [2,*] and Peter R. Ogilby [1,*]

[1] Department of Chemistry, Aarhus University, DK-8000 Aarhus, Denmark; ciaran_mcl@hotmail.com (C.K.M.); mibr@chem.au.dk (M.B.)

[2] Department of Chemistry, National and Kapodistrian University of Athens, 15771 Athens, Greece; helen.kotroni@gmail.com (E.K.); rotasgiorgos@hotmail.com (G.R.)

* Correspondence: vougiouk@chem.uoa.gr (G.C.V.); progilby@chem.au.dk (P.R.O.)

Received: 19 August 2020; Accepted: 7 September 2020; Published: 10 September 2020

Abstract: Fluorescein, and derivatives of fluorescein, are often used as fluorescent probes and sensors. In systems where pH is a variable, protonation/deprotonation of the molecule can influence the pertinent photophysics. Fluorination of the xanthene moiety can alter the molecule's pK_a such as to render a probe whose photophysics remains invariant over a wide pH range. Di-fluorination is often sufficient to accomplish this goal, as has been demonstrated with compounds such as Oregon Green in which the xanthene moiety is symmetrically difluorinated. In this work, we synthesized a non-symmetrical difluorinated analog of Oregon Green which we call Athens Green. We ascertained that the photophysics and photochemistry of Athens Green, including the oxygen-dependent photophysics that results in the sensitized production of singlet oxygen, $O_2(a^1\Delta_g)$, can differ appreciably from the photophysics of Oregon Green. Our data indicate that Athens Green will be a more benign fluorescent probe in systems that involve the production and removal of $O_2(a^1\Delta_g)$. These results expand the available options in the toolbox of fluorescein-based fluorophores.

Keywords: singlet oxygen; fluorescent probe; photobleaching

1. Introduction

Fluorescein, and many of its derivatives, have long been recognized as useful fluorescent probes [1]. This includes their use in a variety of biological imaging experiments [2]. In this regard, the light emitted is at a readily detected wavelength (~500 nm), the quantum yields of emission are large (>0.9), the molecules are generally photostable, and they do not sensitize the production of singlet molecular oxygen, $O_2(a^1\Delta_g)$, in appreciable yield. Although mechanisms of fluorophore photobleaching are often complicated and depend on the molecule's structure and whether or not molecular oxygen is present in the system, it is acknowledged that $O_2(a^1\Delta_g)$ can be a key intermediate in this regard [3–7]. Thus, a low yield of sensitized $O_2(a^1\Delta_g)$ production not only helps mitigate photobleaching, but it also helps to minimize the extent to which the fluorescein perturbs the system in which it is used as a probe by minimizing the $O_2(a^1\Delta_g)$-mediated oxidative degradation of other molecules.

Xanthene-based molecules such as fluorescein have a feature that influences their use as a fluorescent probe: pH-dependent protonation/deprotonation alters properties of the molecule. In this way, for example, the extent of aggregation and intermolecular binding [8,9], the magnitude of the fluorescence quantum yield [10–13], and the yield of photosensitized $O_2(a^1\Delta_g)$ production [12,14] all depend on whether the molecule is in its dianion, monoanion, or neutral form (Figure 1). Although more

complicated schemes can be presented to illustrate the pH-dependent structures of fluoresceins [15,16], the equilibria shown in Figure 1 are sufficient for our current discussion.

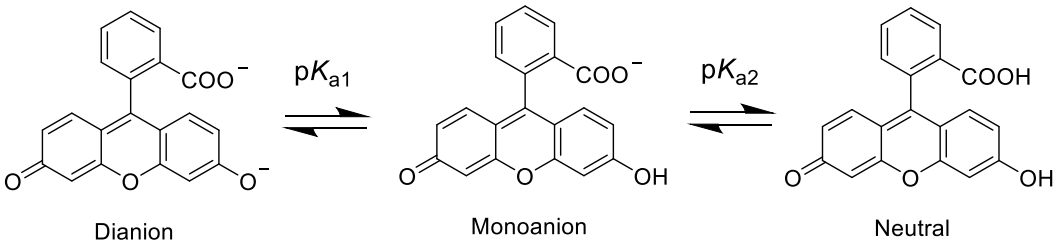

Figure 1. Scheme illustrating the equilibrium between the neutral, monoanionic, and dianionic forms of fluorescein.

It has long been recognized that fluorinating the xanthene ring in fluorescein and its derivatives is one way to change the equilibrium constants shown in Figure 1, particularly that between the dianion and monoanion upon which much of the photophysics in common aqueous solutions depends [12,14–18]. Specifically, upon replacing the xanthene hydrogen atoms with more electronegative fluorine atoms, one stabilizes the dianion yielding a smaller pK_{a1} value. In this way, one can use the fluorescein derivative over a wider pH range without a protonation-dependent change in photophysical properties. Fluorination of a chromophore/fluorophore can also result in a molecule that is more stable to photooxidative degradation, partly due to a decrease in the yield of photosensitized $O_2(a^1\Delta_g)$ production and partly to a decreased reactivity with electrophiles such as $O_2(a^1\Delta_g)$ [7,12,14,19].

Although a variety of fluorinated fluorescein derivatives have been synthesized and studied over the years [12,14–18], the molecules produced have almost exclusively had the fluorine atoms symmetrically disposed on the xanthene moiety of the molecule. Representative examples include Oregon Green and 4′,5′-difluoro Oregon Green (Figure 2). To our knowledge, there is only one report on a non-symmetrical 2′,4′-difluorofluorescein, and this work focused on synthesis rather than on photophysical studies [20].

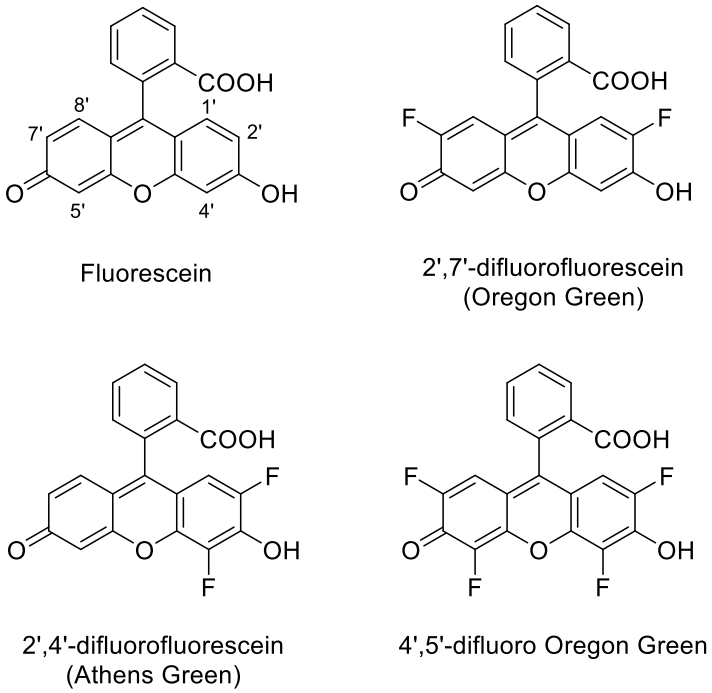

Figure 2. Chemical structures of the compounds investigated in this study. The standard numbering system for fluorescein is shown in the top left.

Most importantly, and again to our knowledge, studies that compare the photophysical properties of symmetrical and non-symmetrical fluorinated fluorescein derivatives have yet to be performed. The potential for appreciable differences in these properties, due to the anticipated changes in electron density distribution, is sufficient justification for a study of selected photophysical parameters. However, even if photophysical differences are small, the synthetic procedures used to prepare a given fluorescein derivative may be more easily realized for the non-symmetrical isomer and thus provides additional justification for this work. For example, it is acknowledged that the synthesis of the tetra-fluorinated fluorescein derivative called Aarhus Sensor Green is challenging [14], and it would be beneficial if other more readily prepared fluorinated derivatives have photophysical properties that are just as acceptable.

From a general synthetic point of view, there are only a few reports on the preparation of non-symmetrically functionalized fluorescein derivatives. The latter has generally been achieved via two consecutive Friedel–Crafts acylation reactions with substituted phenols [20,21]. The main problem in these syntheses is the undesired formation of symmetrical derivatives [22]. As such, in itself, this is an issue that deserves attention.

For the present work, we provide a study on the synthesis of the non-symmetrical 2′,4′-difluorofluorescein. Moreover, we compare selected photophysical properties of this non-symmetrical derivative to those obtained from the symmetrical 2′,7′-isomer (i.e., Oregon Green), the tetra-fluorinated fluorescein (i.e., 4′,5′-difluoro Oregon Green), and fluorescein itself (Figure 2). Given the tautomerization shown in Figure 3 and the standard numbering system shown in Figure 2, the 2′,4′-difluorofluorescein could also be identified as 5′,7′-difluorofluorescein.

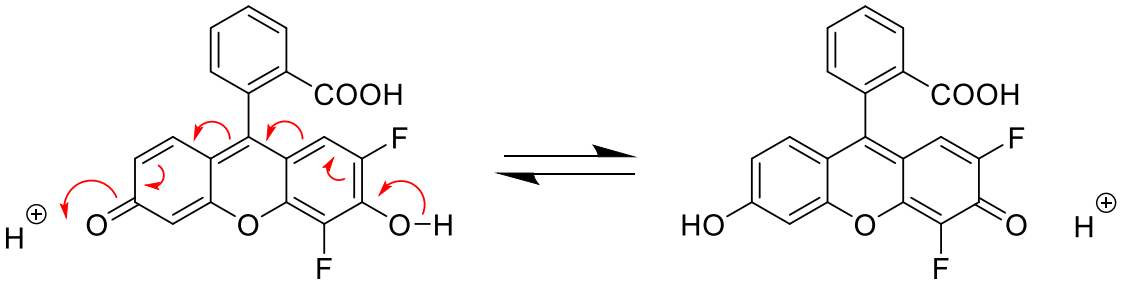

Figure 3. Tautomerization that shows the effective equivalence of the 2′,4′- and 5′,7′-difluorofluoresceines.

It has become a convention when making new fluorescein derivatives to name the compound according to the place in which it was first made. Alongside the proper IUPAC nomenclature, this reversion to "common" nomenclature certainly facilitates conversations about the respective compounds. Thus, we now have Tokyo Green [23], Oregon Green [17], Pennsylvania Green [18], Singapore Green [24], Granada Green [25], and Aarhus Green [12], for example. In this spirit, we refer to our new 2′,4′-difluorofluorescein as Athens Green (Figure 2).

2. Results and Discussion

2.1. Synthesis of Athens Green

As shown in Scheme 1, we approached the synthesis of the non-symmetric difluoro derivative through two independent stepwise Friedel–Crafts reactions of resorcinol (**R**), 2,4-difluororesorcinol (**diFR**), and phthalic anhydride (**PA**). We prepared **diFR** in four steps from 2,3,4,5-tetrafluoronitrobenzene [14].

In this way, the fluorine-free ketone **1** was prepared using the standard $AlCl_3$-mediated procedure. To add the fluorine atoms, **1** was then subjected to a second Friedel-Crafts reaction with **diFR**, this time using methanesulfonic acid both as the catalyst and the solvent [20,22]. Published reports indicate that similar reactions were performed at low temperature to avoid the formation of symmetric fluoresceins stemming from competing Friedel-Crafts reactions [20,22]. In our hands, the reaction between **1** and **diFR** afforded non-fluorinated fluorescein **4** as the main product, together with other unidentified products and only traces of **3** and **5** (Scheme 1). Performing the reaction at 0 °C, or ambient

temperature, or by using excess **diFR**, did not change the outcome. In a different approach, we prepared ketone **2** using the Friedel-Crafts reaction between **PA** and **diFR**. The low nucleophilicity of the latter required heating to 120 °C to obtain **2** in moderate yield. Reaction with **R** then afforded the desired non-symmetrical difluoride **3** in low but reproducible yield.

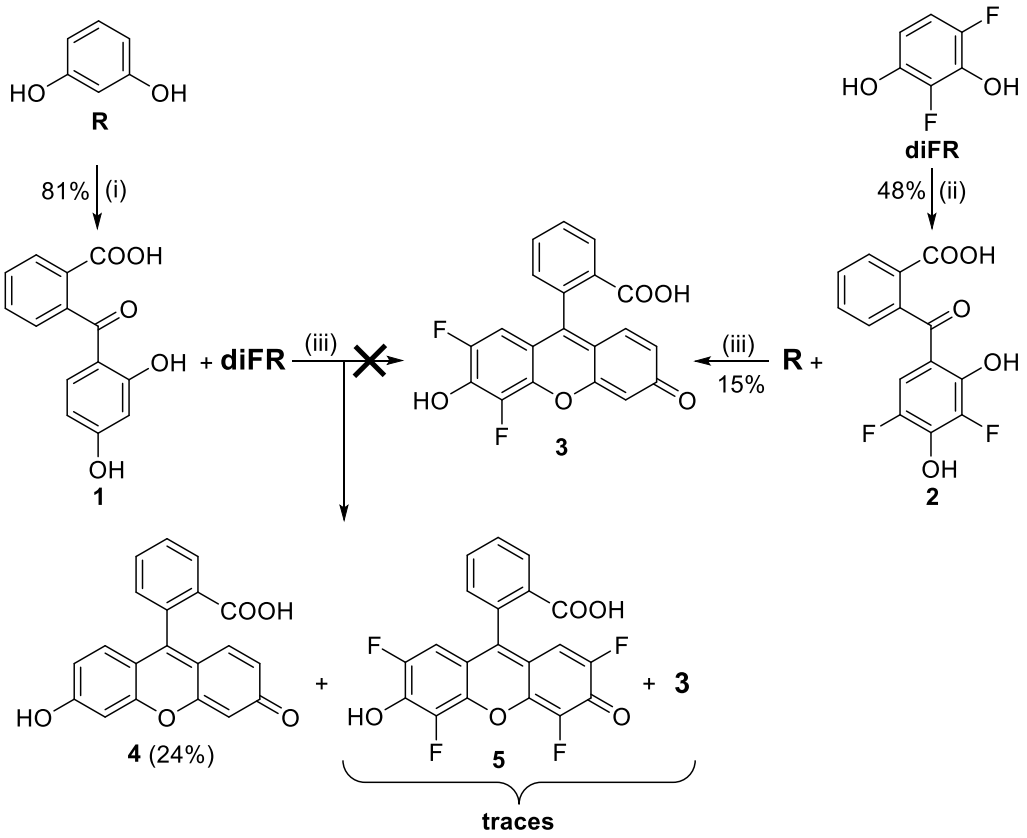

Scheme 1. Synthetic approaches used to produce Athens Green, **3**. Reagents and conditions: (i) **PA**, $AlCl_3$, CH_3NO_2, room temperature, (ii) **PA**, $AlCl_3$, CH_3NO_2, 120 °C, (iii) a) CH_3SO_3H, b) Et_3N. The yields of each reaction are shown as percentages.

We propose the mechanism shown in Scheme 2, which can rationalize why the reaction of ketone **1** with **diFR** principally produces fluorescein **4**, while the reaction of ketone **2** and **R** affords mainly difluorinated fluorescein **3** (i.e., Athens Green). It is first important to recognize that, because we work under acidic conditions, we should consider all reactions shown in Scheme 2 as equilibria (i.e., Friedel-Crafts and reverse Friedel-Crafts reactions). Thus, for example, in the reaction of ketone **1** and **diFR**, formation of the Friedel-Crafts product **7** will compete with the formation of **R** and **PA** via a reverse Friedel-Crafts reaction. In both the Friedel-Crafts and reverse Friedel-Crafts reactions, similar arenium carbocation intermediates are formed ($\mathbf{CC_a}$ and $\mathbf{CC_b}$ in Scheme 2), either from the nucleophilic attack of the aromatic ring on a carbonyl carbon or a proton. These carbocations may be deprotonated (Friedel-Crafts) or decarbonylated (reverse Friedel-Crafts). When substituted with the electronegative fluorine atoms (X = F in Scheme 2), the carbocations are less stable. As such, if arenium carbocation formation is the rate-determining step of both the Friedel-Crafts and the reverse Friedel-Crafts reactions, as expected for a typical electrophilic aromatic substitution reaction [26], any reaction involving **diFR**, either as reactant (Friedel-Crafts) or product (reverse Friedel-Crafts) should be less favorable and, thus, slower. Therefore, the reaction of **2** with **R** is the best way to obtain the non-symmetrical difluoride **3** (i.e., Athens Green).

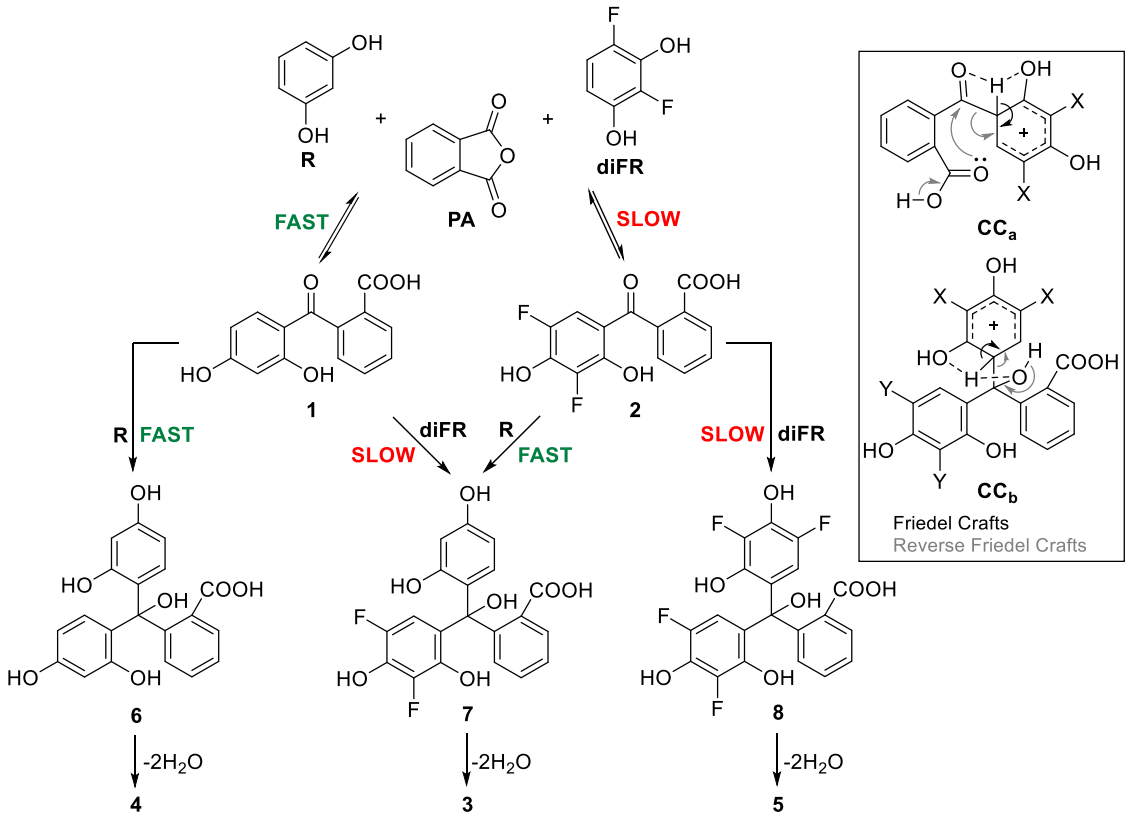

Scheme 2. Proposed mechanistic representation of the formation of fluoresceins **3**, **4,** and **5** (i.e., Athens Green, fluorescein, and 4′,5′-difluoro Oregon Green, respectively).

2.2. *Photophysics and Photochemistry*

Photophysical measurements were performed using both D_2O- and H_2O-based solutions. The rationale for this is the desire to perform selected oxygen-dependent studies in D_2O where $O_2(a^1\Delta_g)$ has a much longer lifetime than in H_2O [27,28].

2.2.1. Absorption and Fluorescence Spectra

The absorption and fluorescence spectra of our four compounds dissolved in a phosphate-buffered D_2O solution (pD = 7.8 = pH + 0.4 [29,30]) are shown in Figure 4. As outlined further below, the spectra at this pD mostly reflects the properties of the dianion of each compound.

Our results show that fluorination generally results in a bathochromic shift of the band maximum in both the absorption and emission spectra (Figure 4 and Table 1). This observation is consistent with data published on related compounds [20]. Most interestingly, however, the spectra of the symmetrical 2′,7′-difluoro compound (i.e., Oregon Green) are not appreciably different from those of fluorine-free fluorescein, whereas the spectra of the non-symmetrical 2′,4′-difluoro derivative (i.e., Athens Green) are noticeably red-shifted by ~10 nm. Fluorination in all four positions to form 4′,5′-difluoro Oregon Green results in a further red-shift of ~10 nm.

As expected, changing the pH/pD of the solution causes pronounced spectral and intensity changes in the absorption and emission spectra of all compounds. This is illustrated in Figure 5A for Athens Green where acidification results in a ~50 nm blue shift of the principal absorption band in the visible region of the spectrum. Although a corresponding spectral shift is not observed in the fluorescence spectrum of Athens Green, acidification results in an appreciable decrease in the fluorescence intensity (Figure 5B).

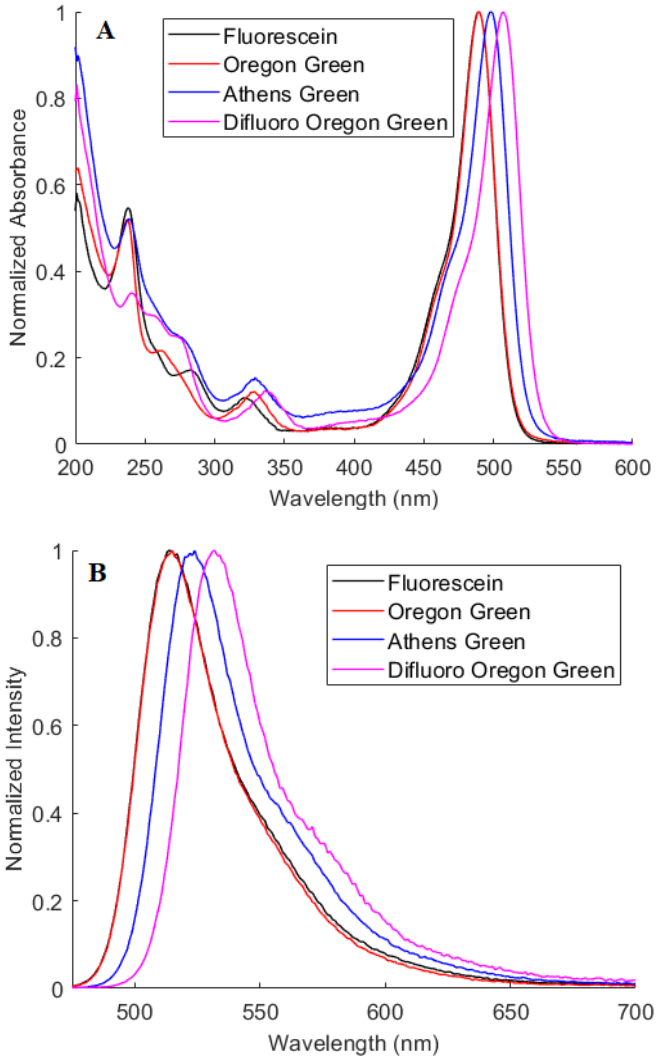

Figure 4. Normalized absorption (**A**) and fluorescence (**B**) spectra of the four compounds dissolved in D_2O-PBS (pD = 7.8). Spectra recorded from H_2O-PBS solutions are identical. Note that the spectra for fluorescein and Oregon Green are similar (black and red lines, respectively).

Table 1. Extinction coefficients at the peak of the absorption band (ε_{max}), the absorption ($\lambda_{max}{}^{abs}$), and fluorescence ($\lambda_{max}{}^{fl}$) band maxima, and fluorescence (φ_{fl}) quantum yields, all recorded from air-saturated PBS buffered solutions at pH = 7.4 or pD = 7.8.

Compound	ε_{max} ($M^{-1}cm^{-1}$)	$\lambda_{max}{}^{abs}$ (nm)	$\lambda_{max}{}^{fl}$ (nm)	φ_{fl}	
	D_2O/H_2O [a]	D_2O/H_2O [a]	D_2O/H_2O [a]	H_2O	D_2O
Fluorescein [b]	73000 ± 2900	490 ± 1	514 ± 1	0.92 ± 0.02	0.98 ± 0.02
Oregon Green	81000 ± 2700	490 ± 1	514 ± 1	Not measured	0.92 ± 0.03
Athens Green	82800 ± 3300	498 ± 1	523 ± 1	0.86 ± 0.02	0.91 ± 0.02
Difluoro Oregon Green	86700 ± 2900	507 ± 1	532 ± 1	Not measured	0.88 ± 0.02

[a] The extinction coefficients and peak maxima are the same in both H_2O and D_2O-based solutions. [b] In a PBS solution at pH = 7.4 or pD = 7.8, some fraction of the fluorescein molecules exist as monoanions. For all other compounds, the pK_a values are sufficiently small that these data principally reflect the characteristics of the dianion). The extinction coefficient we obtain for fluorescein at this pH value is smaller than what has been reported at pH 9.0 (90,000 $M^{-1}cm^{-1}$) [17].

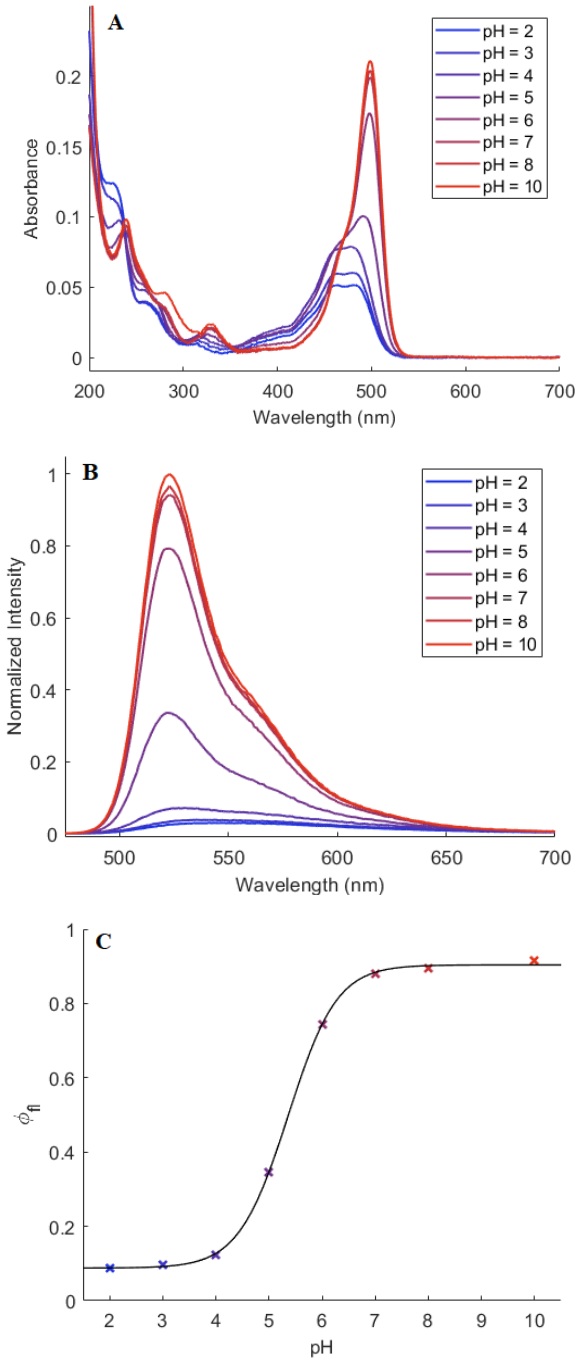

Figure 5. (**A**) Absorption spectra, (**B**) fluorescence spectra, and (**C**) fluorescence quantum yield, φ_{fl}, of Athens Green in H_2O recorded as a function of pH. For the latter, errors on a given point are approximately 5% of the φ_{fl} magnitude shown. For the fluorescence data, the excitation wavelength was 470 nm, and the spectra in panel B were normalized for pH-dependent changes in the sample absorbance at 470 nm. The φ_{fl} titration curve yields a pK_{a1} value of 5.3 ± 0.2. The second pK_a value is not evident from these data likely because of similar fluorescence and absorption properties of the monoanionic and neutral forms of Athens Green.

2.2.2. Lifetimes of the Fluorescent State

Time-resolved fluorescence experiments were used to quantify excited singlet state lifetimes as a function of the oxygen concentration in our aqueous solutions (Table 2). In general, the values of ~4–5 ns thus obtained are consistent with what is expected based on data from related fluoresceins [31,32].

For all compounds, the lifetimes are shorter (Table 2) and the fluorescence quantum yields are smaller (Table 1) for molecules dissolved in H_2O as opposed to D_2O. This phenomenon has been independently observed for fluorescein and was interpreted to indicate that the O–H bond in the solvent plays an important role as an energy acceptor in the process of fluorescein internal conversion [31]. A similar argument has long been presented for an analogous H_2O/D_2O solvent isotope effect on the lifetime of $O_2(a^1\Delta_g)$ [28,33].

Table 2. Lifetimes of the fluorescent state, τ_{fl}, in H_2O-PBS and D_2O-PBS as a function of the concentration of dissolved oxygen.

Compound	τ_{fl} (ns) [a]					
	H_2O-PBS			D_2O-PBS		
	N_2	Air	O_2	N_2	Air	O_2
Fluorescein	4.28	4.26	4.25	4.75	4.69	4.60
Oregon Green	4.30	4.30	4.23	4.52	4.53	4.40
Athens Green	4.46	4.34	4.30	4.94	4.87	4.74
Difluoro Oregon Green	4.06	4.00	3.90	4.91	4.84	4.76

[a] Errors on all numbers are ±0.05 ns.

There is no apparent correlation between the lifetime and the extent of xanthene fluorination. However, for all molecules, the lifetime appears to systematically get shorter as the oxygen concentration in the sample is increased (Table 2). Given the magnitude of the changes observed and errors of our measurements, however, we are hesitant to use this observation to extract a rate constant for the quenching of the excited singlet state by oxygen. Nevertheless, given that the concentration of dissolved oxygen in water is low [34], and that we are seeing a systematic effect of oxygen on lifetimes with a magnitude of 4–5 ns, implies that this rate constant is at or near the diffusion-controlled limit of ~10^{10} s^{-1} M^{-1}. This is the conventional expectation for the quenching of a fluorescent state by oxygen [35,36].

2.2.3. Fluorescence Quantum Yields

The decrease in the fluorescence intensity of Athens Green upon acidification (Figure 5B) reflects a corresponding decrease in the fluorescence quantum yield (φ_{fl}). The latter is an expected observation based on data from other fluorescein derivatives in which protonation of the highly fluorescent dianion yields the weakly fluorescent monoanion [12,20]. The resultant titration curve (Figure 5C) yields a pK_{a1} value of 5.3 ± 0.2 for Athens Green in H_2O. This pK_a value for the non-symmetrical difluoro derivative is slightly larger than those reported for the symmetrical difluoro derivative Oregon Green (4.8 and 5.1) [15,17]. This difference in pK_a values is consistent with what we independently recorded in our $O_2(a^1\Delta_g)$ experiments (vide infra).

For data recorded under alkaline conditions, our fluorescence quantum yield of ~0.9 for Athens Green (Table 1, Figure 5C) is larger than the quantum yield (φ_{fl} = 0.63) reported for the related non-symmetrical difluorinated compound in which the pendant aryl group has two carboxyl groups instead of one [20]. Moreover, we obtain a p*K*a value of 5.3 for Athens Green, whereas a p*K*a value of 5.6 was obtained for the dicarboxylated analog [20].

These data recorded from different difluoro derivatives indicate that presumed subtle structural changes, including those on moieties removed from the xanthene core, can have appreciable photophysical consequences.

2.2.4. Sensitized Production of $O_2(a^1\Delta_g)$

Based on the data presented above, we expect only small yields of fluorescein-sensitized $O_2(a^1\Delta_g)$ production at pH > ~7. Specifically, we observe comparatively large quantum yields of fluorescence (Table 1) and that oxygen does not effectively quench the excited singlet state to promote intersystem crossing (i.e., the longer-lived triplet state would be a suitable $O_2(a^1\Delta_g)$ precursor). However, upon

acidification, both monoanionic and neutral fluoresceins can sensitize the production of $O_2(a^1\Delta_g)$ in greater yield [12,14,37]. Moreover, even if produced in only small amounts, $O_2(a^1\Delta_g)$ can lead to the photooxidative bleaching of the fluorophore [6,7] which, in turn, can result in the production of an efficient $O_2(a^1\Delta_g)$ sensitizer [37,38]. It is thus incumbent upon us to quantify pH-dependent yields of $O_2(a^1\Delta_g)$ sensitized by these fluorescein derivatives.

The ability of our compounds to sensitize the production of $O_2(a^1\Delta_g)$ was quantified by monitoring the characteristic 1275 nm phosphorescence of $O_2(a^1\Delta_g)$ in time-resolved experiments. Because the lifetime of $O_2(a^1\Delta_g)$, τ_Δ, is longer in D_2O (67 µs) than in H_2O (3.5 µs) [28], it is an advantage to perform these experiments in D_2O solutions where the quantum efficiency of $O_2(a^1\Delta_g)$ phosphorescence is correspondingly greater. Moreover, with a longer $O_2(a^1\Delta_g)$ lifetime, it becomes easier to discriminate between $O_2(a^1\Delta_g)$ removal and $O_2(a^1\Delta_g)$ production; the latter generally occurs with time constants of ~3–5 µs in aqueous solutions due to the slow rate of sensitizer deactivation by the comparatively low concentration of oxygen [28,39].

Quantum yields of $O_2(a^1\Delta_g)$ production, φ_Δ, were obtained in the standard way by comparing the intensity of the fluorescein-sensitized $O_2(a^1\Delta_g)$ phosphorescence signal to the corresponding signal from $O_2(a^1\Delta_g)$ produced by a reference sensitizer, using data obtained over a range of incident laser powers [40]. For our present experiments, the reference used was phenalen-1-one-2-sulfonic acid (PNS) [41]. Representative data for Athens Green are shown in Figure 6.

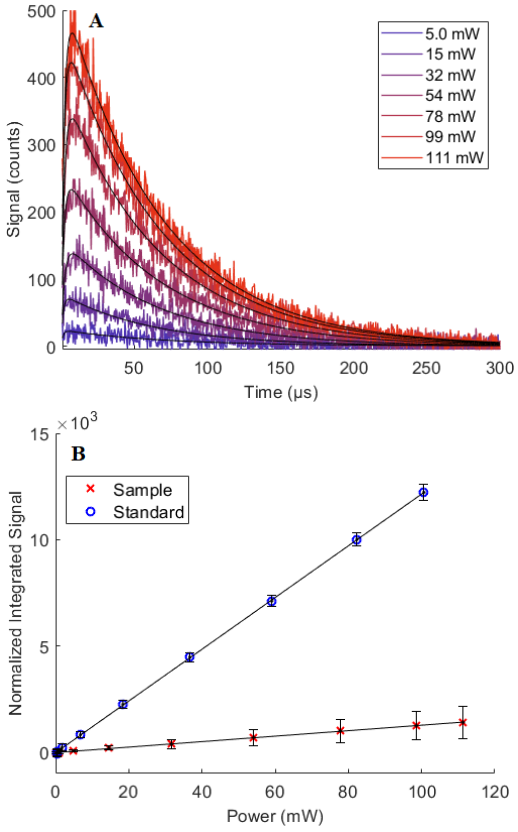

Figure 6. (**A**) Representative time-resolved $O_2(a^1\Delta_g) \rightarrow O_2(X^3\Sigma_g^-)$ phosphorescence traces recorded at 1275 nm upon 420 nm pulsed laser irradiation of Athens Green in air-saturated D_2O at pD = 5.0. For the triplet state photosensitized production of $O_2(a^1\Delta_g)$ in water, where the concentration of oxygen is comparatively low, it is common to discern a rise in the time-resolved signal corresponding to the comparatively slow rate of $O_2(a^1\Delta_g)$ production. Such data are quantified using a difference of two exponential functions [27,39], and this fitting function is superimposed on each kinetic trace. (**B**) The integrated signal amplitude, normalized by the $O_2(a^1\Delta_g)$ lifetime, τ_Δ, and the sample absorbance, plotted as a function of the incident laser power. The slopes of the linear fits are proportional to φ_Δ.

All our compounds sensitize the production of $O_2(a^1\Delta_g)$ in readily detectable amounts. As expected from previous studies [12,14], values of φ_Δ are small under alkaline conditions where the fluorescein dianion predominates (Table 3). This is consistent with the large quantum yields of fluorescence and oxygen-independent fluorescence lifetimes observed under the same conditions (vide supra). Saturating the solution with oxygen does not significantly increase φ_Δ indicating that most of the expected precursor to $O_2(a^1\Delta_g)$, the fluorescein triplet state, is quenched by oxygen under air-saturated conditions (Table 3).

Table 3. Singlet oxygen quantum yields, φ_Δ, recorded from air- and oxygen-saturated D_2O-PBS solutions.

	φ_Δ [a]			
Compound	**pD = 7.8**		**pD = 5**	
	Air-Saturated	**O_2-Saturated**	**Air-Saturated**	**O_2-Saturated**
Fluorescein [b]	0.04	0.05	0.16 [c]	0.19 [c]
Oregon Green	0.02	0.03	0.28	0.34
Athens Green	0.02	0.04	0.12	0.14
Difluoro Oregon Green	0.05	0.07	0.06	0.06

[a] Errors on all numbers are ±0.01. [b] At pD = 7.8, a small fraction of the fluorescein molecules exist in monoanionic form. For all other compounds, the p*K*a is sufficiently low that the data principally reflect the effects of the dianion (see Table 4). [c] Measured at pD = 6 (i.e., the maximum of the φ_Δ versus pD plot; see Figure 7).

Table 4. Relative $O_2(a^1\Delta_g)$ quantum yields, φ_Δ, in air-saturated D_2O for the neutral (n), monoanionic (ma), and dianionic (da) species, and the corresponding pK_a values for the interconversion between them, as obtained through Equation (1). [a.]

Compound	φ_Δ^{da}	**pK_{a1}**	φ_Δ^{ma}	**pK_{a2}**	φ_Δ^{n}
Fluorescein	0.03 ± 0.01	7.1 ± 0.3	0.17 ± 0.01	4.2 ± 0.2	0.15 ± 0.01
Oregon Green	0.02 ± 0.01	5.4 ± 0.2	0.34 ± 0.02	3.7 ± 0.2	0.24 ± 0.02
Athens Green	0.01 ± 0.01	5.7 ± 0.2	0.08 ± 0.01	3.4 ± 0.2	0.05 ± 0.01
Difluoro Oregon Green	0.04 ± 0.01	4.1 ± 0.2	0.03 ± 0.01	<2 [b]	- [b]

[a.] The numbers shown here were obtained from fits of Equation (1) to plots of the singlet oxygen yield against pD (e.g., Figure 7). Recall also the expected difference of ~0.4 units in p*K*a values for experiments performed in H_2O and D_2O [30]. [b.] The second p*K*a value of difluoro Oregon Green falls below our investigated pD range.

Upon acidification of fluorescein and both difluorofluoresceins, φ_Δ increases to a maximum value at a pD where the monoanion dominates the equilibria (Figure 7). Thereafter, further acidification results in a slight decrease in φ_Δ. Most importantly, this pD-dependent increase in the $O_2(a^1\Delta_g)$ yield is comparatively small for Athens Green (from ~0.02 to 0.12 in an air-saturated solution), whereas it is much larger for Oregon Green (from ~0.02 to 0.28, likewise in an air-saturated solution).

Although pD dependent changes in φ_Δ for difluoro Oregon Green are very small (Table 3) and are arguably smaller than our absolute accuracy in determining φ_Δ, the relative changes obtained upon systematically decrementing the pD show a clear decrease in φ_Δ upon acidification to form the mono anion (Figure 7B). As such, the pD dependent behavior of this tetrafluorinated fluorescein is distinctly different from that of the difluoro and fluorine-free analogs with respect to $O_2(a^1\Delta_g)$ production. Based on the data that we currently have available, we are not able to explain this observation. Moreover, we are likewise currently hesitant to speculate on the origins of the more pronounced difference in φ_Δ between the non-symmetrical and symmetrical difluorofluoresceins. In themselves, these observations are fodder for a detailed independent study.

At any given pD, the measured value of the $O_2(a^1\Delta_g)$ quantum yield, φ_Δ^{meas}, will reflect contributions from the dianionic (da), the monoanionic (ma), and the neutral (n) species, and we can model the pD-dependence of φ_Δ^{meas} shown in Figure 7 with the function in Equation (1).

$$\varphi_\Delta^{meas} = \varphi_\Delta^{da} + \frac{\varphi_\Delta^{ma} - \varphi_\Delta^{da}}{1 + 10^{pD - pK_{a1}}} + \frac{\varphi_\Delta^{n} - \varphi_\Delta^{ma}}{1 + 10^{pD - pK_{a2}}} \quad (1)$$

In this treatment, $\varphi_\Delta{}^{da}$, $\varphi_\Delta{}^{ma}$, and $\varphi_\Delta{}^{n}$ do not reflect the actual quantum yields of $O_2(a^1\Delta_g)$ production because we do not account for pD-dependent changes in the absorbance of each species. Nevertheless, $\varphi_\Delta{}^{meas}$ represents the weighted average of relative quantum yields from the respective pD-dependent components. In Table 4, we show parameters obtained from the application of Equation (1) to our pD-dependent data shown in Figure 7. Note that pK_a values obtained from D_2O-based solutions are not expected to be identical to those obtained from H_2O-based solutions [30].

The results shown in Table 4, confirm that fluorination decreases the pK_a values of fluorescein. More importantly, the relative values of φ_Δ obtained through Equation (1) indicate that under all conditions, non-symmetric Athens Green produces appreciably less $O_2(a^1\Delta_g)$ than the symmetric analog, Oregon Green.

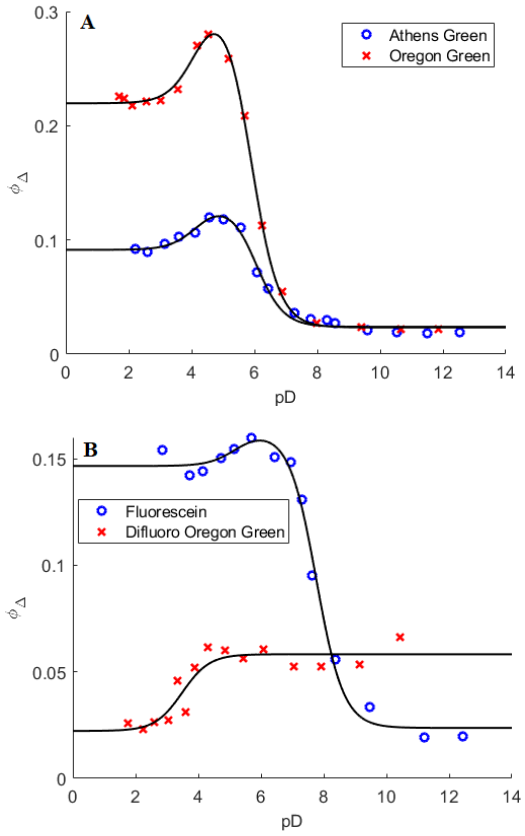

Figure 7. The $O_2(a^1\Delta_g)$ quantum yield, φ_Δ, plotted as a function of the pD in air-saturated D_2O-based solutions for (**A**) Athens Green and Oregon Green, and (**B**) fluorescein and difluoro Oregon Green. The solid lines are numerical fits to Equation (1). Differences in p*K*a and φ_Δ values are apparent in these plots, and the pertinent numbers are shown in Table 4. For a given data point, the error is approximately 10% of the value shown.

2.3. Rate Constants for the Fluorescein-Mediated Removal of $O_2(a^1\Delta_g)$

To complement pD-dependent measurements of $O_2(a^1\Delta_g)$ production sensitized by the fluorescein derivatives, we set out to monitor pD-dependent rate constants for $O_2(a^1\Delta_g)$ removal by these same derivatives. For this latter exercise, it is useful to quantify not just the rate constant for total removal, k_{total}, but to perform experiments that distinguish the rate of removal via the fluorescein-mediated physical deactivation of $O_2(a^1\Delta_g)$ to $O_2(X^3\Sigma_g{}^-)$, k_{phys}, from the rate of $O_2(a^1\Delta_g)$ removal via a chemical reaction with the fluorescein, k_{chem}. Although the photobleaching mechanisms of fluorescein derivatives depend on whether oxygen is present or not [3,5–7], the magnitudes of k_{phys} and k_{chem} are certainly relevant for systems in which $O_2(a^1\Delta_g)$ is produced, either by the fluorescein derivative itself or by another chromophore in the system.

2.3.1. Rate Constants for the Total Removal of $O_2(a^1\Delta_g)$

The rate constant for total solute-mediated $O_2(a^1\Delta_g)$ removal, k_{total}, which is the sum of k_{phys} and k_{chem}, is readily obtained from time-resolved $O_2(a^1\Delta_g)$ phosphorescence measurements performed as a function of the solute concentration. This experiment is best performed using a method for $O_2(a^1\Delta_g)$ production that is independent of the solute used to mediate $O_2(a^1\Delta_g)$ removal. To this end, we used Al(III) phthalocyanine tetrasulfonic acid, $AlPcS_4$, as an $O_2(a^1\Delta_g)$ photosensitizer [42]. Like its disulfonated analog, the $AlPcS_4$-sensitized yield of $O_2(a^1\Delta_g)$ will likely depend on pH [43]. For our kinetic experiments, however, this parameter is irrelevant as long as the yield is sufficiently large to yield good $O_2(a^1\Delta_g)$ phosphorescence signals. Most importantly, the absorption spectrum of $AlPcS_4$ is sufficiently red-shifted relative to those of our fluorescein derivatives that, upon irradiation, we avoid exciting the fluorescein itself [44] (also see Supplementary Materials). Representative data from these experiments are shown in Figure 8, and the values of k_{total} thus obtained are shown in Table 5.

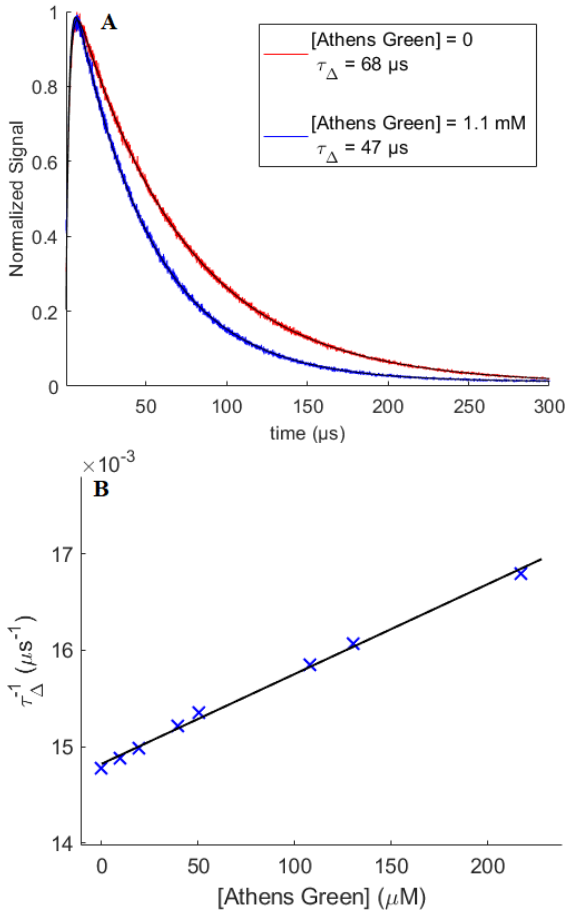

Figure 8. (**A**) Representative time-resolved 1275 nm $O_2(a^1\Delta_g)$ phosphorescence traces recorded upon 670 nm pulsed laser irradiation of $AlPcS_4$ in air-saturated D_2O-PBS at pD = 7.8 in the presence of Athens Green, the concentration of which is shown in the legend. (**B**) The inverse lifetime of $O_2(a^1\Delta_g)$, ${\tau_\Delta}^{-1}$, plotted as a function of the concentration of Athens Green, obtained from experiments such as those shown inFigure 8A. The solid black line is a linear fit to the data, the slope of which yields k_{total}. The size of the symbols in Figure 8B represent the errors on each data point.

2.3.2. Rate Constants for the Removal of $O_2(a^1\Delta_g)$ by Reaction

The magnitude of k_{chem} can be independently determined using experiments in which $O_2(a^1\Delta_g)$-mediated changes in the fluorescein absorption spectra are monitored. The general kinetic approach we used is described elsewhere [45], and representative examples of our data are shown in

Figure 9. For these experiments, we again produced $O_2(a^1\Delta_g)$ upon irradiation of $AlPcS_4$ at 670 nm. We ascertained that, over the period in which appreciable changes in the fluorescein spectra were observed, we saw no change in the $AlPcS_4$ spectrum. Values of k_{chem} thus obtained are shown in Table 5.

Table 5. Rate constants for the interaction with $O_2(a^1\Delta_g)$ measured at two different pD values in air-saturated solutions.

Compound	pD = 7.8				pD = 5			
	k_{total} 10^6 $M^{-1}s^{-1}$	k_{chem} 10^6 $M^{-1}s^{-1}$	k_{phys} [a] 10^6 $M^{-1}s^{-1}$	$\frac{k_{phys}}{k_{chem}}$	k_{total} 10^6 $M^{-1}s^{-1}$	k_{chem} 10^6 $M^{-1}s^{-1}$	k_{phys} [a] 10^6 $M^{-1}s^{-1}$	$\frac{k_{phys}}{k_{chem}}$
Fluorescein	8.5 ± 0.8	2.0 ± 0.3	6.5 ± 1.1	3.3	4 [b]	0.2 [b]	3.8 [b]	19 [b]
Oregon Green	19 ± 2	0.6 ± 0.1	18.4 ± 3.2	31	9.1 ± 0.9	0.39 ± 0.09 [c]	8.7 ± 2.0	22
Athens Green	6.0 ± 0.6	1.7 ± 0.2	4.3 ± 0.7	2.5	3.3 ± 0.3 [d]	0.27 ± 0.06	3.0 ± 0.7	11
Difluoro OG [e]	3.6 ± 0.4	0.8 ± 0.1	2.8 ± 0.5	3.5	-	-	-	-

[a] Obtained from k_{total}–k_{chem}. Given the errors on k_{chem} and k_{phys}, the error on the ratio of k_{phys}/k_{chem} is sufficiently large (~20–25% of the value shown) that we choose to only conclude that physical deactivation of $O_2(a^1\Delta_g)$ is more probable than chemical reaction with $O_2(a^1\Delta_g)$ for these molecules (see text). [b] It was difficult to dissolve a sufficient amount of fluorescein to yield a non-negligible change in the $O_2(a^1\Delta_g)$ lifetime when determining k_{total}. For k_{chem}, we accounted for a non-negligible change in the dark reaction. Thus, the errors on these numbers are large. As with the $O_2(a^1\Delta_g)$ experiments, these experiments were also performed at pD 6. [c] There was a non-negligible dark reaction, and this change was subtracted from the change upon irradiation (see Supplementary Materials). [d] With 1% DMSO by volume. This was required to dissolve enough Athens Green to get an appreciable change in the $O_2(a^1\Delta_g)$ lifetime. [e] Difluoro Oregon Green.

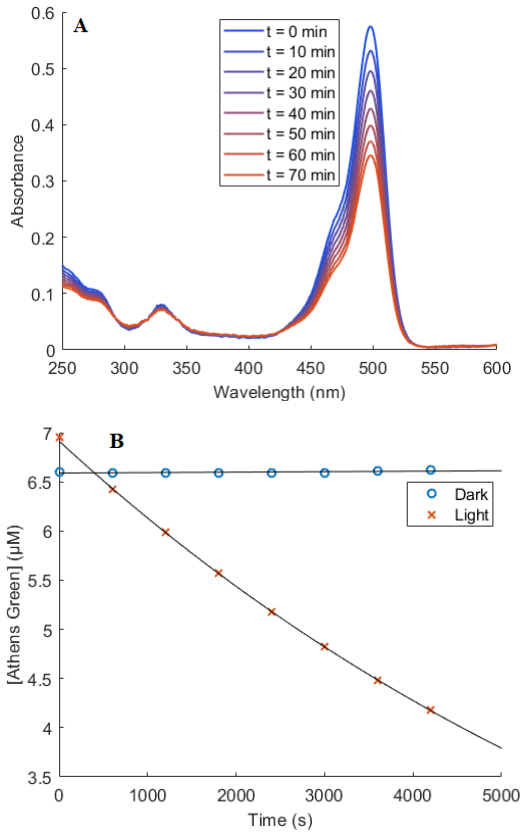

Figure 9. (**A**) Absorption spectra of Athens Green in D_2O-PBS (pD 7.8) recorded as a function of the elapsed irradiation time of the $O_2(a^1\Delta_g)$ sensitizer $AlPcS_4$ at 670 nm. The absorption spectrum of $AlPcS_4$ does not change under these conditions and was subtracted to yield the data shown. (**B**) The concentration of Athens Green as a function of $AlPcS_4$ irradiation time (crosses). An independent sample, kept in the dark and monitored at identical intervals, did not show detectable absorption changes. The solid lines are fits to the pertinent kinetic rate equations for reactions with $O_2(a^1\Delta_g)$ [45]. The size of the symbols in Figure 9B represent the errors on each data point.

2.3.3. Interpreting Relative Changes in the Removal Rate Constants

We first note that, with the change in pD from 7.8 to 5 and the associated protonation of the dianion to yield the monoanion, all of the rate constants for $O_2(a^1\Delta_g)$ removal decrease for both Oregon Green and Athens Green (Table 5). This is arguably expected given that $O_2(a^1\Delta_g)$ is an electrophile, and it is consistent with the general observation that electron-rich molecules are most efficient at removing/deactivating $O_2(a^1\Delta_g)$ [46]. Moreover, our data indicate that Oregon Green and Athens Green both predominantly remove $O_2(a^1\Delta_g)$ via physical deactivation to $O_2(X^3\Sigma_g^-)$ as opposed to a chemical reaction (i.e., $k_{phys}/k_{chem} > 2$; Table 5). Beyond these similarities, however, and as outlined below, there are clear differences in the rate constants for $O_2(a^1\Delta_g)$ removal by Oregon Green and Athens Green, as there were with the yields of photosensitized $O_2(a^1\Delta_g)$ production (Table 3).

Overall, and irrespective of the pD, Athens Green is a poorer quencher of $O_2(a^1\Delta_g)$ than Oregon Green (i.e., k_{total}(Athens Green) < k_{total}(Oregon Green)). This difference in k_{total} principally reflects the respective values of k_{phys} (Table 5). Moreover, of all the fluorescein derivatives we examined, the absolute magnitude of k_{phys} is the largest for Oregon Green. In turn, this results in a k_{phys}/k_{chem} ratio for Oregon Green that is over 10 times greater than that for Athens Green. Of the postulated mechanisms for solute-mediated $O_2(a^1\Delta_g)$ deactivation to $O_2(X^3\Sigma_g^-)$, processes that occur with rate constants of ~10^6–10^7 s^{-1} M^{-1}, as we have for these fluoresceins, focus on the role played by the oxygen-quencher charge-transfer (CT) state [47–50]. The thesis is that, for a compound M that can better donate charge to oxygen, the $M^{+\cdot}O_2^{-\cdot}$ CT state will play a greater role in facilitating the $O_2(a^1\Delta_g)$ → $O_2(X^3\Sigma_g^-)$ transition. Thus, one hypothesis to account for our data is that the M-O_2 CT state for Oregon Green plays a greater role than the corresponding CT state for Athens Green in the process of deactivating $O_2(a^1\Delta_g)$.

Organic dye molecules and fluorophores, including the fluoresceins, photobleach by a variety of mechanisms in oxygen-containing systems [4–7]. These photobleaching reactions are undesired in many microscopy applications where a stable fluorophore is an attribute [51]. This is also true for organic solar cells where a stable light-absorbing compound is desired [52]. Reactions with $O_2(a^1\Delta_g)$ constitute one important channel for such photodegradation. With this in mind, the magnitude of k_{chem} becomes important. Our data indicate that, at pD 7.8, the rate constant for the reaction of $O_2(a^1\Delta_g)$ with Athens Green is approximately three times greater than the corresponding rate constant for the reaction of $O_2(a^1\Delta_g)$ with Oregon Green (Table 5). At pD 5, although the difference in k_{chem} for these two molecules becomes negligible, a pronounced dark reaction contributes to the bleaching of Oregon Green whereas Athens Green is stable in the dark (see Supplementary Materials). An attempt to interpret these observations must include a detailed study of the reaction products and this, in itself, will be a challenging independent study. Although the judicious addition of substituent groups to Athens Green could reduce reactivity with $O_2(a^1\Delta_g)$, the absolute value of k_{chem} is already small enough that such reactions will not preclude the use of Athens Green as a fluorescent probe in many applications. This latter point is reinforced by the fact that the yield of $O_2(a^1\Delta_g)$ produced upon irradiation of Athens Green is less than that of Oregon Green (Table 3).

Thus, our data clearly show that, if a benign fluorescence probe is desired, Athens Green is a better choice than Oregon Green; Oregon Green will initiate and interfere with an $O_2(a^1\Delta_g)$-mediated process to a greater extent than Athens Green.

3. Conclusions

We synthesized a non-symmetrical difluorinated derivative of fluorescein, calling this compound Athens Green. Its symmetrical difluorinated complement is the well-established compound called Oregon Green. We ascertained that the oxygen-dependent photophysics and photochemistry of Athens Green differ appreciably from that of Oregon Green. In particular, Athens Green produces less $O_2(a^1\Delta_g)$ upon irradiation and does not remove $O_2(a^1\Delta_g)$ as efficiently as Oregon Green. As such, Athens Green would arguably be a more benign fluorescent probe in photosystems that involve $O_2(a^1\Delta_g)$. On a more general level, our results show that the site of fluorination in a given molecule can have a profound

effect on photophysical properties pertinent to the use of that molecule as a sensor. Thus, given the advantages of using a fluorinated fluorescein derivative over using fluorescein itself (i.e., the fluorinated compound can be used over a wider pH range), and given that fluorescein itself has already been established as a useful probe in a wide range of disciplines [1], Athens Green should be a welcome addition to the toolbox of fluorescent probes.

4. Materials and Methods

*4.1. Synthesis of 2-(2,4-dihydroxybenzoyl)benzoic Acid (**1**)*

Prepared as described in the literature [53]. Aluminum trichloride (1.08 g, 8.1 mmol) was added to a solution of **PA** (400 mg, 2.7 mmol) and **R** (273 mg, 2.7 mmol) in dry nitrobenzene (6 mL) under argon, and the mixture was degassed (Ar bubbling) for 30 min. The mixture was stirred for 24 h, decanted into a vigorously stirred 1:1 biphasic mixture of 0.5 N HCl (aq)/hexane (30 mL), the obtained mixture was stirred for 2 h, and the precipitate was filtered and washed with water and hexane. The resulting impure product was crystallized from a methanol/water mixture to afford **1** as an off-white powder (564 mg, 81%): ^{1}H-NMR (200 MHz, DMSO-d_6) δ 13.22 (bs, 1H, COOH), 12.25 (s, 1H, OH), 10.75 (s, 1H, OH), 8.04–7.96 (m, 1H, H-6), 7.75–7.59 (m, 2H, H-4, H-5), 7.42 (dd, *J* = 7.1, 1.4 Hz, 1H, H-3), 6.92 (d, *J* = 8.6 Hz, 1H, H-6′), 6.35–6.25 (m, 2H, H-3′, H-5′). ^{13}C NMR (50 MHz, DMSO-d_6) δ 200.54, 166.76, 164.93, 164.17, 140.08, 134.84, 132.43, 130.07, 129.81, 129.42, 127.52, 113.33, 108.34, 102.51. ES-HRMS m/z for $C_{14}H_7F_2O_5$ $[M-H]^-$: calcd. 293.03, found 293.03.

*4.2. Synthesis of 2-(3,5-difluoro-2,4-dihydroxybenzoyl)benzoic Acid (**2**)*

Aluminum trichloride (1.08 g, 8.1 mmol) was added in a solution of **PA** (400 mg, 2.7 mmol) and 2,4-difluororesorcinol (395 mg, 2.7 mmol) in dry nitrobenzene (10 mL) under argon, and the resulting mixture was degassed (Ar bubbling) for 30 min. The mixture was stirred at 120 °C for 24 h, decanted into a vigorously stirred 1:1 biphasic mixture of 1 N HCl (aq)/hexane (40 mL), the mixture was stirred for 2 h, and the precipitate was filtered and washed with water and hexane. The resulting impure product was crystallized from a methanol/water mixture to afford **2** as an off-white powder (420 mg, 53%): ^{1}H-NMR (200 MHz, CD_3OD) δ 8.11 (app d, *J* = 7.2 Hz, 1H, H-6), 7.77–7.59 (m, 2H, H-4, H-5), 7.39 (app d, *J* = 7.1 Hz, 1H, H-3), 6.55 (app d, *J* = 11.0, 1H, H-6′). ^{19}F-NMR (188 MHz, CD_3OD) δ -146.43 (dd, *J* = 11.0, 6.3 Hz, 1F, F-5′), -160.65 (app d, *J* = 6.3 Hz, 1F, F-6′). ^{13}C-NMR (75 MHz, CD_3OD) δ 202.77, 168.47, 150.17 (dd, *J* = 12.6, 2.3 Hz), 145.87 (dd, *J* = 236.2, 4.3 Hz), 143.16 (dd, *J* = 17.9, 12.8 Hz), 142.02 (dd, *J* = 241.5, 5.4 Hz), 141.20, 133.66, 131.56, 131.14, 130.61, 128.40, 113.33 (dd, *J* = 20.6, 2.9 Hz), 112.74 (dd, *J* = 6.7, 2.3 Hz). ES-HRMS m/z for $C_{14}H_7F_2O_5$ $[M-H]^-$: calcd. 293.0262, found 293.0239.

*4.3. Synthesis of 2-(5,7- Difluoro-6-hydroxy-3-oxo-3h-xanthen-9-yl)benzoic Acid (Athens Green, **3**)*

A mixture of **2** (200 mg, 0.68 mmol) and **R** (69 mg, 0.68 mmol) in methanesulfonic acid (3 mL) was stirred under argon for 4 h. The mixture was decanted into crushed ice (60 mL), and the resulting mixture was brought to room temperature and extracted with ethyl acetate (3 × 20 mL). The combined organic phases were washed with water, dried and the solvent was evaporated. The residue was suspended in water (10 mL), basified with triethylamine (pH≈10), and the resulting dark solution was refluxed for 10 min and left to cool down. The mixture was acidified with 1N HCl (pH≈2), extracted with ethyl acetate (3 × 20 mL), the combined organic phases were washed with water, dried and the solvent was evaporated. The residue was subjected to column chromatography (EtOAc/petroleum ether 10–100%) yielding **3** (51 mg, 15%) as an orange powder. ^{1}H-NMR (200 MHz, DMSO-d_6) δ 10.51 (bs, 2H, OH), 8.01 (d, *J* = 7.3 Hz, 1H, H-6), 7.85–7.67 (m, 2H, H-4, H-5), 7.33 (d, *J* = 7.2 Hz, 1H, H-3), 6.76 (s, 1H, H-4′), 6.64–6.55 (m, 1H, H-1′, H-2′), 6.40 (dd, *J* = 10.9, 2.2 Hz, 1H, H-8′). ^{19}F-NMR (188 MHz, DMSO-d_6) δ-136.93 (bs, 1F, F-5′, -154.06 (bs, 1F, F-7′). ^{13}C-NMR (75 MHz, DMSO-d_6) δ 168.78, 160.26, 151.96, 151.57, 148.83 (dd, *J* = 238.6 Hz), 140.93 (dd, *J* = 243.8, 6.6 Hz), 137.92 (d, *J* = 10.1 Hz), 137.02 (m),

136.04, 130.76, 129.50, 126.46, 125.50, 124.63, 113.85, 109.67 (d, J = 7.6 Hz), 109.45, 108.54 (dd, J = 20.9, 3.1 Hz), 102.79, 82.58. ES-HRMS m/z for $C_{20}H_9F_2O_5$ $[M\text{-}H]^-$: calcd. 367.0418, found 367.0429.

4.4. Materials

Fluorescein was obtained from Sigma-Aldrich (>95%) and 2′,7′-difluorofluorescein (i.e., Oregon Green 488^{TM}) was obtained from Thermo Fisher Scientific (>95%). The tetrafluoro substituted fluorescein derivative, 4′,5′-difluoro Oregon Green, was prepared using the procedure of Sun et al. [17]. Al(III) phthalocyanine tetrasulfonic acid ($AlPcS_4$, >95%) was obtained from Frontier Scientific and Rhodamine 6G (R6G, >99%) from Sigma Aldrich, and both were used as received. The sulfonated derivative of 1H-phenalenone (PNS) was synthesized as described by Nonell et al. [54]. Heavy water (D_2O, 99.9% D) was obtained from EurisoTop, whereas H_2O was purified by filtration (Milli-Q system by Millipore Corporation).

H_2O- and D_2O-based phosphate-buffered saline (PBS) solutions were prepared using commercially available PBS tablets (Sigma-Aldrich). The pH of H_2O-solutions was adjusted using hydrochloric acid (HCl) and sodium hydroxide (NaOH), whereas the pD of D_2O-based solutions was adjusted with deuterochloric acid (DCl) and sodium deuteroxide (NaOD). The respective acids and bases were obtained from Sigma-Aldrich.

The tendency of fluorescein and Oregon Green to undergo excited-state proton transfer reactions has been documented [16,55]. If a suitable proton donor or acceptor (such as a phosphate buffer) is present, this can affect the photophysics. Hence, care must be exercised with the amount of any substance used to control the pH of our solutions. In all cases, we used the minimal amount of acid/base necessary to obtain a given pH, or we used the minimal amount of PBS (Total phosphate concentration = 0.01 M, [NaCl] = 0.137 M, [KCl] = 2.7 mM). In this regard, a phosphate concentration of 10 mM is low, compared to what is generally necessary to affect fluorescein singlet state photophysics [55]. Furthermore, control experiments using buffered and un-buffered solutions showed no difference in selected photophysical properties at identical pH values. Hence, we conclude that, under our conditions, the data are not sensitive to excited state reactions involving the buffer.

4.5. Methods

The spectroscopic instruments and procedures we use to (a) monitor excited states, (b) generate and detect $O_2(a^1\Delta_g)$, and (c) follow the ensuing $O_2(a^1\Delta_g)$-induced chemistry have been previously described [45,56,57]. All reported quantum yields of $O_2(a^1\Delta_g)$ production were measured using PNS in D_2O-PBS as the standard (φ_Δ = 0.97 ± 0.06) [41]. Fluorescence quantum yields were determined using Rhodamine 6G in D_2O-PBS (φ_{fl} = 0.98 ± 0.015) or H_2O-PBS (φ_{fl} = 0.92 ± 0.02) as the standard [31,58]. The pH of D_2O solutions, as measured with a pH-meter (Knick pH-matic), were corrected using the general formula pD = pH + 0.4 [29].

Supplementary Materials: The following are available online at http://www.mdpi.com/1424-8220/20/18/5172/s1: NMR spectra, pD-dependent absorption and fluorescence spectra for difluoro Oregon Green, absorption spectra of $AlPcS_4$, and plots used to determine k_{chem}.

Author Contributions: Conceptualization, G.C.V., G.R. and P.R.O.; methodology, G.C.V., G.R., M.B. and P.R.O.; validation, G.C.V., G.R., M.B., C.K.M. and P.R.O.; formal analysis, E.K., G.R., M.B., C.K.M. and P.R.O.; writing—original draft preparation, G.R., M.B. and P.R.O.; writing—review and editing, G.C.V. and P.R.O.; supervision, G.C.V., G.R. and P.R.O; project administration, G.C.V. and P.R.O.; funding acquisition, G.C.V. and P.R.O. All authors have read and agreed to the published version of the manuscript.

Funding: Grants from the Danish Research Council, the Danish Ministry of Higher Education in Science (LaserLab.dk), and the Special Account for Research Grants of the National and Kapodistrian University of Athens (research projects 14872 and 16294) supported the work described herein.

Acknowledgments: The authors thank Mikkel Due Petersen for the preparation of 4′,5′-difluoro Oregon Green.

Conflicts of Interest: The authors declare no conflict of interest.

References

1. Lakowicz, J.R. *Principles of Fluorescence Spectroscopy*; Springer: New York, NY, USA, 2006.
2. Robertson, T.A.; Bunel, F.; Roberts, M.S. Fluorescein derivatives in intravital fluoresence imaging. *Cells* **2013**, *2*, 591–606. [CrossRef] [PubMed]
3. Widengren, J.; Rigler, R. Mechanisms of photobleaching investgated by fluorescence correlation spectroscopy. *Bioimaging* **1996**, *4*, 149–157. [CrossRef]
4. Song, L.; Hennik, E.J.; Young, I.T.; Tanke, H.J. Photobleaching kinetics of fluorescein in quantitative fluorescence microscopy. *Biophys. J.* **1995**, *68*, 2588–2600. [CrossRef]
5. Song, L.; Varma, C.A.G.O.; Verhoeven, J.W.; Tanke, H.J. Influence of the triplet excited state on the photobleaching kinetics of fluorescein in microscopy. *Biophys. J.* **1996**, *70*, 2959–2968. [CrossRef]
6. Zheng, Q.; Jockusch, S.; Zhou, Z.; Blanchard, S.C. The contribution of reactive oxygen species to the photobleaching of organic fluorophores. *Photochem. Photobiol.* **2014**, *90*, 448–454. [CrossRef]
7. Silva, E.F.F.; Pimenta, F.M.; Pedersen, B.W.; Blaikie, F.H.; Bosio, G.N.; Breitenbach, T.; Westberg, M.; Bregnhøj, M.; Etzerodt, M.; Arnaut, L.G.; et al. Intracellular singlet oxygen photosensitizers: On the road to solving the problems of sensitizer degradation, bleaching and relocalization. *Integr. Biol.* **2016**, *8*, 177–193. [CrossRef]
8. Valdes-Aguilera, O.; Neckers, D.C. Aggregation phenomena in xanthene dyes. *Acc. Chem. Res.* **1989**, *22*, 171–177. [CrossRef]
9. Lavis, L.D.; Rutkoski, T.J.; Raines, R.T. Tuning the pKa of fluorescein to optimize binding assays. *Anal. Chem.* **2007**, *79*, 6775–6782. [CrossRef]
10. Klonis, N.; Sawyer, W.H. Spectral properties of the prototropic forms of fluorescein in aqueous solution. *J. Fluoresc.* **1996**, *6*, 147–157. [CrossRef]
11. Martin, M.M.; Lindqvist, L. The pH dependence of fluorescein fluorescence. *J. Lumin.* **1975**, *10*, 381–390. [CrossRef]
12. Holmehave, J.; Pedersen, S.K.; Jensen, H.H.; Ogilby, P.R. Aarhus Green: A tetrafluoro-substituted derivative of fluorescein. *ARKIVOC* **2015**, *2015*, 52–64.
13. Han, J.; Burgess, K. Fluorescent indicators for intracellular pH. *Chem. Rev.* **2010**, *110*, 2709–2728. [CrossRef] [PubMed]
14. Pedersen, S.K.; Holmehave, J.; Blaikie, F.H.; Gollmer, A.; Breitenbach, T.; Jensen, H.H.; Ogilby, P.R. Aarhus Sensor Green: A fluorescent probe for singlet oxygen. *J. Org. Chem.* **2014**, *79*, 3079–3087. [CrossRef] [PubMed]
15. Mchedlov-Petrossyan, N.O.; Vodolazkaya, N.A.; Gurina, Y.A.; Sun, W.-C.; Gee, K.R. Medium effects on the prototropic equilibria of fluorescein fluoro derivatives in true and organized solution. *J. Phys. Chem. B* **2010**, *114*, 4551–4564. [CrossRef] [PubMed]
16. Orte, A.; Crovetto, L.; Talavera, E.M.; Boens, N.; Alvarez-Pez, J. Absorption and emission study of 2′,7′-difluorofluorescein and its excited-state buffer-mediated proton exchange reactions. *J. Phys. Chem. A* **2005**, *109*, 734–747. [CrossRef]
17. Sun, W.-C.; Gee, K.R.; Klaubert, D.H.; Haugland, R.P. Synthesis of fluorinated fluoresceins. *J. Org. Chem.* **1997**, *62*, 6469–6475. [CrossRef]
18. Mottram, L.F.; Boonyarattanakalin, S.; Kovel, R.E.; Peterson, B.R. The Pennsylvania green fluorophore: A hybrid of oregon green and tokyo green for the construction of hydrophobic and ph-insensitive molecular probes. *Org. Lett.* **2006**, *8*, 581–584. [CrossRef]
19. Renikuntla, B.R.; Rose, H.C.; Eldo, J.; Waggoner, A.S.; Armitage, B.A. Improved photostability and fluorescence properties through polyfluorination of a cyanine dye. *Org. Lett.* **2004**, *6*, 909–912. [CrossRef]
20. Hammershøj, P.; Kumar, E.K.P.; Harris, P.; Andresen, T.L.; Clausen, M.H. Facile large-scale sythesis of 5- and 6-carboxyfluoresceins: Application for the Preparation of new fluorescent dyes. *Eur. J. Org. Chem.* **2015**, *2015*, 7301–7309. [CrossRef]
21. Burdette, S.C.; Frederickson, C.J.; Bu, W.; Lippard, S.J. ZP4, an improved neuronal Zn^{2+} sensor of the zinpyr family. *J. Am. Chem. Soc.* **2003**, *125*, 1778–1787. [CrossRef]
22. Lukhtanov, E.A.; Vorobiev, A.V. Mild synthesis of asymmetric 2′-carboxyethyl-substituted fluoresceins. *J. Org. Chem.* **2008**, *73*, 2424–2427. [CrossRef]
23. Urano, Y.; Kamiya, M.; Kanda, K.; Ueno, T.; Hirose, K.; Nagano, T. Evolution of fluorescein as a platform for finely tunable fluorescence probes. *J. Am. Chem. Soc.* **2005**, *127*, 4888–4894. [CrossRef]

24. Li, J.; Yao, S.-Q. "Singapore Green": A new fluorescent dye for microarray and bioimaging applications. *Org. Lett.* **2009**, *11*, 405–408. [CrossRef]
25. Martinez-Peragon, A.; Miguel, D.; Orte, A.; Mota, A.J.; Ruedas-Rama, M.J.; Justicia, J.; Alvarez-Pez, J.M.; Cuerva, J.M.; Crovetto, L. Rational design of a new fluorescent "on/off" xanthene dye for phosphate detection in live cells. *Org. Biomol. Chem.* **2014**, *12*, 6432–6439. [CrossRef] [PubMed]
26. Butler, A.R. Electrophilic Aromatic Substitution. In *Organic Reaction Mechansims*; Capon, B., Rees, C.W., Eds.; John Wiley and Sons: Chichester, UK, 1969.
27. Ogilby, P.R. Singlet oxygen: There is indeed something new under the sun. *Chem. Soc. Rev.* **2010**, *39*, 3181–3209. [CrossRef]
28. Bregnhøj, M.; Westberg, M.; Minaev, B.F.; Ogilby, P.R. Singlet oxygen photophysics in liquid solvents: Converging on a unified picture. *Acc. Chem. Res.* **2017**, *50*, 1920–1927. [CrossRef] [PubMed]
29. Covington, A.K.; Paabo, M.; Robinson, R.A.; Bates, R.G. Use of the glass electrode in deuterium oxide and the relation between the standardized pD (pa_D) scale and the operational pH in heavy water. *Anal. Chem.* **1968**, *40*, 700–706. [CrossRef]
30. Krezel, A.; Bal, W. A formula for correlating p*K*a values determined in D_2O and H_2O. *J. Inorg. Biochem.* **2004**, *98*, 161–166. [CrossRef]
31. Magde, D.; Wong, R.; Seybold, P.G. Fluorescence quantum yields and their relation to lifetimes of rhodamine 6G and fluorescein in nine solvents: Improved absolute standards for quantum yields. *Photochem. Photobiol.* **2002**, *75*, 327–334. [CrossRef]
32. Alvarez-Pez, J.M.; Ballesteros, L.; Talavera, E.M.; Yguerabide, J. Fluorescein excited-state proton exchange reactions: Nanosecond emission kinetics and correlation with steady-state fluorescence intensity. *J. Phys. Chem. A* **2001**, *105*, 6320–6332. [CrossRef]
33. Thorning, F.; Jensen, F.; Ogilby, P.R. Modeling the effect of solvents on nonradiative singlet oxygen deactivation: Going beyond weak coupling in intermolecular electronic-to-vibrational energy transfer. *J. Phys. Chem. B* **2020**, *124*, 2245–2254. [CrossRef] [PubMed]
34. Battino, R.; Rettich, T.R.; Tominaga, T. The solubility of oxygen and ozone in liquids. *J. Phys. Chem. Ref. Data* **1983**, *12*, 163–178. [CrossRef]
35. Ware, W.R. Oxygen quenching of fluorescence in solution: An experimental study of the diffusion process. *J. Phys. Chem.* **1962**, *66*, 455–458. [CrossRef]
36. Montalti, M.; Credi, A.; Prodi, L.; Gandolfi, M.T. *Handbook of Photochemistry*; CRC Press: Boca Raton, FL, USA, 2006.
37. Gollmer, A.; Arnbjerg, J.; Blaikie, F.H.; Pedersen, B.W.; Breitenbach, T.; Daasbjerg, K.; Glasius, M.; Ogilby, P.R. Singlet oxygen sensor green®: Photochemical behavior in solution and in a mammalian cell. *Photochem. Photobiol.* **2011**, *87*, 671–679. [CrossRef] [PubMed]
38. Pimenta, F.M.; Jensen, R.L.; Breitenbach, T.; Etzerodt, M.; Ogilby, P.R. Oxygen-dependent photochemistry and photophysics of "miniSOG", a protein-encased flavin. *Photochem. Photobiol.* **2013**, *89*, 1116–1126. [CrossRef]
39. Snyder, J.W.; Skovsen, E.; Lambert, J.D.C.; Poulsen, L.; Ogilby, P.R. Optical detection of singlet oxygen from single cells. *Phys. Chem. Chem. Phys.* **2006**, *8*, 4280–4293. [CrossRef]
40. Scurlock, R.D.; Mártire, D.O.; Ogilby, P.R.; Taylor, V.L.; Clough, R.L. Quantum yield of photosensitized singlet oxygen ($a^1\Delta_g$) production in solid polystyrene. *Macromolecules* **1994**, *27*, 4787–4794. [CrossRef]
41. Marti, C.; Jürgens, O.; Cuenca, O.; Casals, M.; Nonell, S. Aromatic ketones as standards for singlet molecular oxygen $O_2(^1\Delta_g)$ photosensitization. Time-resolved photoacoustic and near-IR emission studies. *J. Photochem. Photobiol. A. Chem.* **1996**, *97*, 11–18. [CrossRef]
42. Keir, W.F.; Land, E.J.; MacLennan, A.H.; McGarvey, D.J.; Truscott, T.G. Pulsed Radition studies of photodynamic sensitizers: The nature of DHE. *Photochem. Photobiol.* **1987**, *46*, 587–589. [CrossRef]
43. Ostler, R.B.; Scully, A.D.; Taylor, A.G.; Gould, I.R.; Smith, T.A.; Waite, A.; Phillips, D. The effect of pH on the photophysics and photochemistry of di-sulphonated aluminum phthalocyanine. *Photochem. Photobiol.* **2000**, *71*, 397–404. [CrossRef]
44. Dhami, S.; de Mello, A.J.; Rumbles, G.; Bishop, S.M.; Phillips, D.; Beeby, A. Phthalocyanine fluorescence at high concentration: Dimers or reabsorption effect? *Photochem. Photobiol.* **1995**, *61*, 341–346. [CrossRef]
45. Bregnhøj, M.; Krægpøth, M.V.; Sørensen, R.J.; Westberg, M.; Ogilby, P.R. Solvent and heavy-atom effects on the $O_2(X^3\Sigma_g^-)$ - $O_2(b^1\Sigma_g^+)$ absorption transition. *J. Phys. Chem. A* **2016**, *120*, 8285–8296. [CrossRef] [PubMed]

46. Wilkinson, F.; Helman, W.P.; Ross, A.B. Rate constants for the decay and reactions of the lowest electronically excited singlet state of molecular oxygen in solution. An expanded and revised compilation. *J. Phys. Chem. Ref. Data* **1995**, *24*, 663–1021. [CrossRef]
47. Schweitzer, C.; Schmidt, R. Physical mechanisms of generation and deactivation of singlet oxygen. *Chem. Rev.* **2003**, *103*, 1685–1757. [CrossRef] [PubMed]
48. Clennan, E.L.; Noe, L.J.; Szneler, E.; Wen, T. Hydrazines: New charge-transfer physical quenchers of singlet oxygen. *J. Am. Chem. Soc.* **1990**, *112*, 5080–5085. [CrossRef]
49. Paterson, M.J.; Christiansen, O.; Jensen, F.; Ogilby, P.R. Overview of theoretical and computational methods applied to the oxygen-organic molecule photosystem. *Photochem. Photobiol.* **2006**, *82*, 1136–1160. [CrossRef]
50. Jensen, P.-G.; Arnbjerg, J.; Tolbod, L.P.; Toftegaard, R.; Ogilby, P.R. Influence of an intermolecular charge-transfer state on excited-state relaxation dynamics: Solvent effect on the methylnaphthalene-oxygen system and its significance for singlet oxygen production. *J. Phys. Chem. A* **2009**, *113*, 9965–9973. [CrossRef]
51. Pawley, J.B. (Ed.) *Handbook of Biological Confocal Microscopy*; Springer: New York, NY, USA, 2006.
52. Cheng, P.; Zhan, X. Stability of organic solar cells: Challenges and strategies. *Chem. Soc. Rev.* **2016**, *45*, 2544–2582. [CrossRef]
53. Smith, G.A.; Metcalfe, J.C.; Clarke, S.D. The design and properties of a series of calcium indicators which shift from rhodamine-like to fluorescein-like fluorescence on binding calcium. *J. Chem. Soc. Perkin Trans.* **1993**, *2*, 1195–1204. [CrossRef]
54. Nonell, S.; Gonzalez, M.; Trull, F.R. 1H-Phenalen-1-one-2-sulfonic acid: An extremely efficient singlet molecular oxygen sensitizer for aqueous media. *Afinidad* **1993**, *448*, 445–450.
55. Paredes, J.M.; Crovetto, L.; Rios, R.; Orte, A.; Alvarez-Pez, J.M.; Talavera, E.M. Tuned lifetime, at the ensemble and single molecule level, of a xanthenic fluorescent dye by means of a buffer-mediated excited state proton exchange reaction. *Phys. Chem. Chem. Phys.* **2009**, *11*, 5400–5407. [CrossRef] [PubMed]
56. Westberg, M.; Bregnhøj, M.; Etzerodt, M.; Ogilby, P.R. Temperature sensitive singlet oxygen photosensitization by LOV-derived fluorescent flavoproteins. *J. Phys. Chem. B* **2017**, *121*, 2561–2574. [CrossRef] [PubMed]
57. Arnbjerg, J.; Johnsen, M.; Frederiksen, P.K.; Braslavsky, S.E.; Ogilby, P.R. Two-photon photosensitized production of singlet oxygen: Optical and optoacoustic characterization of absolute two-photon absorption cross sections for standard sensitizers in different solvents. *J. Phys. Chem. A* **2006**, *110*, 7375–7385. [CrossRef] [PubMed]
58. Brouwer, A.M. Standards for photoluminescence quantum yield measurements in solution (IUPAC Technical Report). *Pure Appl. Chem.* **2011**, *83*, 2213–2228. [CrossRef]